

# A Numerical Study of Scattering from an Object Above a Rough Surface

Joel T. Johnson

Department of Electrical Engineering and ElectroScience Laboratory

The Ohio State University

205 Dreese Laboratories

2015 Neil Ave

Columbus, OH 43210

(614) 292-1593, (614) 292-7297 FAX

johnson@ee.eng.ohio-state.edu

## ABSTRACT

A numerical model is applied in a Monte Carlo study of scattering from a three dimensional penetrable object above a lossy dielectric rough interface. The model is based on an iterative method of moments solution for equivalent electric and magnetic surface current densities on the rough interface and equivalent volumetric electric currents in the penetrable object. Both time and frequency domain results are investigated to illustrate the relative importance of coherent and incoherent scattering effects. Results show that a four-path model using a reduced reflection coefficient can be reasonable for coherent scattering predictions, and that incoherent scattering in the combined object-surface problem can be significantly different than that obtained with the rough surface alone.

*Keywords:* rough surface scattering, radar cross section, electromagnetic scattering

# 1 Introduction

Electromagnetic scattering from objects is affected by the surrounding medium. Many realistic geometries involve objects in the presence of the Earth surface, which is often modeled as a planar dielectric boundary [1]-[4]. However, roughness on the Earth surface can potentially modify object scattering returns from those with a flat surface, particularly in cases where the roughness size becomes larger than a fraction of the electromagnetic wavelength. Analysis of these problems is complicated by the many possible scattering interactions between the rough surface and object; at present, approximate analytical solutions exist only in the small roughness limit [5]-[9].

Recent works have explored numerical solutions of the combined object/rough surface scattering problem [10]-[15], but have concentrated primarily on two dimensional scattering problems to reduce computational complexity. The majority of previous numerical studies have also been directed toward studies of scattering from objects beneath a rough surface for application to ground penetrating radar problems. Substantial motivation also exists, however, for studying problems in which objects are located above a rough surface, as demonstrated in [15]-[17] among other references.

In this paper, a numerical study of scattering from a three dimensional penetrable object located above a lossy dielectric rough interface is performed to provide an illustration of some of the coherent and incoherent scattering effects which can occur. A Monte Carlo simulation is used to obtain scattered field statistics as a function of frequency from 2 to 5 GHz, and results are illustrated in both the frequency and time domains to clarify the scattering physics. Results show that a “four-path” model [4] can remain reasonable for prediction of total coherent scattered fields if a rough surface reflection coefficient [18] is employed. An examination of incoherent scattered fields shows that significant differences can be obtained from those obtained in the presence of the rough surface alone.

The next section briefly reviews the numerical model employed in the study, and Section 3 describes the particular problem for which simulations are performed. Computational issues are discussed in Section 4, and results are presented in Section 5.

## 2 Numerical model

Figure 1 illustrates the basic geometry considered in this paper: a dielectric object with relative complex permittivity  $\epsilon_3$  is located above a rough interface  $z = f(x, y)$  between free space and a dielectric medium with relative complex permittivity  $\epsilon_2$ . The numerical model applied to solve this problem is an iterative method of moments solution for single frequency induced volumetric currents in the dielectric object and induced electric and magnetic surface currents on the rough interface. A point matching formulation is applied, and matrix multiply computations required in the iterative method are accelerated through use of the canonical grid method [19]-[20] and the discrete dipole approach [21]-[22] to compute surface to surface and object to object point couplings, respectively, in  $O(N \log N)$ , where  $N$  is the number of surface or object sampling points. A standard iterative method (the “Bi-conjugate gradient stabilized” (BiCG-stab) algorithm [23]) is used on the combined object/surface matrix equation, and the system is preconditioned through a “flat surface” approximation for surface to surface contributions and a low accuracy DDA solution for object to object contributions. The model is described in detail in [24], where an example of scattering from an object located below a rough interface is provided.

The rough surface profiles used in the study are realizations of a Gaussian random process and for simplicity are chosen to have an isotropic Gaussian correlation function. The resulting surface statistics are described completely by the surface rms height  $h$  and correlation length  $l$ . Due to the statistical nature of this problem, scattered field results obtained from an ensemble of surface realizations are considered. While a large number of realizations is desirable for more accurate estimates of scattered field statistics, computational issues described in Section 4 limit the current study to twenty realizations. Convergence tests with the obtained data show that average cross sections estimates should be accurate to within approximately 3 dB.

Because the rough interface modeled in the simulation is of finite size, a “tapered wave” incident field is used to avoid surface edge scattering effects. Incidence angles of 0 and 45 degrees from normal incidence are considered in this paper, and the respective tapered wave formulations are provided in [25] and [26]. The tapered waves used in the study are chosen so that the object is well within the

3 dB spot size of the incident field while approximately 60 dB incident field attenuation is obtained at surface edges. Tests of tapered wave influence in the flat surface limit have been performed in [4] through comparison with a plane wave incidence halfspace Green's function numerical solution [27]. Results of the comparison show only slight differences (within 1.5 dB) between tapered wave and plane wave radar cross sections obtained from object and object/surface interaction effects. However, note that direct surface backscattering at normal incidence is strongly influenced by tapered wave parameters; for this reason, only incoherent surface backscattering at normal incidence will be presented. Scattered fields in the study are calculated both for the combined object/rough surface problem and the rough surface only problem, so that rough surface scattering effects can be "separated" from object and object/surface interaction effects if desired.

Due to the presence of both object and distributed source (the rough surface) scatterers, total radar cross sections obtained are also dependent on the rough surface area illuminated by the incident tapered wave. For example, in the limit of a very large "spot size" incident field, rough surface scattering effects become more likely to dominate object scattering effects due to the larger surface area illuminated. Thus it should be noted that the results presented apply only for the particular incident field used. However, tests with larger tapered wave spot sizes showed only slight changes in object and object/surface interaction cross sections.

Consideration of the primary scattering effects of this problem suggests that coherent scattered fields (neglecting the direct surface reflection at normal incidence) should resemble those obtained for an object above a flat surface in the small roughness limit, and those obtained for an object in free space in the large roughness limit. A four-path model [4] based on image theory and a single scattering interaction with the object can be developed to describe this process by including the standard rough surface reflection coefficient modification [18] for fields which encounter the rough surface. Incoherent scattered fields should be caused both by direct surface backscattering and by object/surface interaction effects. The four-path model suggests that the latter are likely to be dominated by paths which involve a single bistatic scatter from the object combined with near specular scattering from the rough surface. However, since incoherent scattering from the rough

surface is distributed through a range of angles, incoherent object/surface interaction effects can be very complex and difficult to describe completely. Examination of frequency and time domain results in Section 5 however will give some indication as to the most important contributions.

### 3 Example problem

A dielectric rectangular box with dimensions 7.62 cm by 7.62 cm by 2.54 cm (thickness) and relative permittivity  $\epsilon_3 = 3 + i0.03$  is used as the object in this study. The center of the box is located 8.89 cm above the rough interface between free space and a medium with relative permittivity  $\epsilon_2 = 5 + i1.25$ . Scattering for this geometry is to be determined for a field incident at either 0 or 45 degrees from normal incidence at sixteen frequencies from 2 to 5 GHz. A rough surface correlation length of 3.58 cm and surface rms heights of 3.58 mm or 1 cm are used, so that the surfaces range from slightly rough at the lowest frequency ( $kh = 0.15$  or  $0.42$ , respectively, where  $k$  is the electromagnetic wavenumber) to slightly to moderately rough at the highest frequency ( $kh = 0.375$  or  $1.05$ , respectively). However, rms slopes for these surfaces are approximately 8 degrees and 22 degrees, respectively, making the larger height surface exceed the limitations of standard perturbation theory [28]. Surface-only backscattered fields will be compared with results from the first two terms of the small slope approximation (SSA) [29] calculated in a separate SSA Monte Carlo simulation following the procedure described in [30].

Time domain scattered fields are obtained from frequency swept data through an FFT operation preceded by multiplication with a Kaiser-Bessel window (parameter  $\beta = 3$ ) to reduce side-lobe levels. Time zero is defined to correspond to the center of the mean level of the rough surface ( $z = 0$ ) in Figure 1, so that object scattering returns occur at negative times. A calculation of expected time delays shows object scattering contributions at approximate times of  $-0.60$  ns and  $-0.42$  ns for 0 and 45 degrees incidence respectively. Surface scattering returns within the 3 dB tapered wave spot at 45 degrees incidence are spread in time from approximately  $-0.7$  ns to  $0.7$  ns. This time spreading of surface clutter at oblique observation angles and its effects on detection of objects has been previously described in [14], [31]. Time domain field statistics are calculated in

terms of the mean and variance of the field envelope as a function of time to clarify the time locations of various coherent and incoherent scattering effects. Of course, rough surface incoherent scattered fields should show no particular time location, but object/surface incoherent interaction effects do contain some time information which can help to indicate the important scattering mechanisms.

## 4 Computational issues

A 1.281 m by 1.281 m surface size is used which ranges from 8.5 to 21.35 free space wavelengths side dimension as the frequency varies from 2 to 5 GHz. The tapered wave 3 dB spot diameter with parameter  $g = 5.333$  is then 28.3 cm so that the object is well within the tapered wave illumination pattern. The interface is sampled into 256 by 256 points, producing a sampling rate of 5.36 points per wavelength in the dielectric medium at the highest frequency; tests with 512 by 512 points in the flat surface limit showed negligible cross section variations. While a smaller number of surface points could be used for the lower frequencies, a constant number of points sampling the rough interface as frequency is varied was chosen for convenience. The resulting number of field unknowns on the interface is 262144. A “strong” bandwidth of 15 points and one canonical grid series term were used in rough surface matrix elements, as described in [24]; single realization tests confirmed that these parameters should provide accurate results for rough surface scattering contributions.

The object is sampled on a 32 by 32 by 8 point grid with step size 3.175 mm (ranging from approximately 1/27 to 1/11 of the wavelength in the object as frequency varies), resulting in a total number of 13824 object unknowns. The combined problem thus contains approximately 276000 unknowns. While this large number of unknowns would be prohibitive for many integral equation based methods, the efficient algorithm applied makes the current study possible.

Although the problem considered can be solved on a PC level platform for a single realization, total computing times for the multiple cases considered in this paper were further reduced through use of IBM SP parallel computing resources at the Maui High Performance Computing Center [32]. Since results as a function of frequency for multiple realizations were of interest, single frequency-single realization calculations were performed on individual nodes of the parallel com-

puter (comparable to PC platforms) to obtain twenty realizations with 16 frequencies between 2 and 5 GHz. Single frequency computing times on a single node ranged from approximately six to fourteen hours depending on frequency, incidence angle, and surface statistics; attempts to optimize computing times have at present not been performed extensively. Four-path model contributions were calculated using an object in free space DDA code [21]-[22] with the same grid as in the combined surface/object code, and synthesized following the procedure described in [4].

## 5 Results

### *A. Frequency domain*

Figure 2 plots average coherent (plot (a)) and incoherent (plot (b)) backscattered co-polarized radar cross sections versus frequency for 0 degrees observation and for both the rms height 3.58 mm and 1 cm cases. Again, direct surface reflections are not included in plot (a). Also included are the corresponding cross sections for the object above a flat surface, as well as predictions for coherent cross sections using the reduced reflection coefficient four-path model. Coherent cross sections for the 3.58 mm rms height surface are very similar to those obtained with the object above a flat surface, while those for the rougher surface are significantly different and approach those for the object in free space. The four-path model is found to perform very well for this case, indicating that its approximations remain reasonable even in the presence of rough surfaces. The success of the four-path model indicates that terms involving more than one object scattering process can be neglected for normal incidence in this problem.

Incoherent cross sections in plot (b) are shown for surface-only contributions (obtained from the surface only numerical solution), combined surface/object total contributions, and object/surface interaction terms (obtained with total fields minus surface only fields.) All of these terms are found to increase with frequency, as expected for these surface statistics since more power from the coherent field is converted to incoherent power at higher frequencies. For the smaller rms height surface, total incoherent scattering contributions remain significantly smaller than coherent returns, while incoherent scattering is larger than coherent scattering at some frequencies for the rougher

surfaces. Surface only backscattering dominates object/surface interaction effects at all frequencies for the rougher surface, but object/surface interaction effects become comparable to surface only scattering at higher frequencies for the smaller height surface.

Figures 3 and 4 illustrate coherent and incoherent scattering returns, respectively, for 45 degrees incidence in  $HH$  (plot (a)) and  $VV$  (plot (b)) polarizations. Polarization differences should be observable in this problem for oblique incidence backscattering due to polarized object scattering and due to the polarization sensitivity of rough surface scattering at oblique angles. Coherent cross sections indeed show significant differences between  $HH$  and  $VV$  returns. Differences of rough surface coherent cross sections from those with a flat surface are less noticeable than in the 0 degrees case, due to the reduced Rayleigh parameters obtained at oblique incidence and smaller differences between the object in free space and object above a flat surface returns at 45 degrees. The accuracy of the four-path model (plotted only for the rougher surface case) is also reduced compared to Figure 2; similar levels of error are observed when comparing four-path and numerical model results with a flat surface. These discrepancies indicate that paths involving more than one object scattering process are more important for oblique paths, as discussed in [4].

Incoherent returns in Figure 4 show that incoherent scattering can be greater than coherent scattering even with the small height surface at some frequencies. Incoherent returns for the larger height surface dominate coherent returns at almost all frequencies for both  $HH$  and  $VV$  polarizations. Again surface incoherent scattering is dominant over object/surface interaction effects for almost all cases, but higher frequency  $HH$  results show a region where object/surface interaction contributions exceed those from the rough surface alone. As stated previously, the four-path model for incoherent scattering suggests that object/surface interaction effects can be dominated by paths involving a bistatic object scattering followed by a near-specular surface scattering. Studies of surface-only incoherent scattering cross sections show large increases in forward scattered fields with frequency at 45 degrees, while backscattered returns increase only slightly or decrease with frequency. Furthermore, the ratio of forward to backscattered incoherent cross sections is greatest for the  $HH$ , smaller rms height surface at the highest frequency, where it approaches 25

dB. Forward to backscattered cross section ratios for all other cases obtain maximum values of 15 dB. Thus, the results obtained support the four-path model idea that both surface backscattered and forward scattered incoherent cross sections are important in combined object/rough surface interaction problems.

A validation of rough surface-only incoherent cross sections is presented in Figure 5, where results at 0 degrees (plot (a)) and 45 degrees (plot (b)) are compared with predictions of the first two terms of the SSA. A Monte Carlo simulation using 100 surface realizations was used to obtain SSA results [30], so that the curves obtained show some residual variations due to the finite number of realizations. Numerical model results are in good general agreement with the SSA, although some differences within approximately 4 dB at the lower frequencies (where the tapered wave causes a larger degree of angular averaging) are observed. Overall the reasonable agreement obtained however validates both the numerical model and the SSA prediction for the surfaces considered.

### *B. Time domain*

Figure 6 presents time domain backscattered field envelopes (in decibels) for 0 degrees incidence in the rms height 3.58 mm (plot (a)) and rms height 1 cm (plot (b)) cases. Both coherent and “incoherent” (i.e. the standard deviation of the field envelope as a function of time) returns are included, as well as returns with the object above a flat surface. Incoherent returns are plotted for total, surface only, and object/surface interaction contributions as well. Coherent returns in Figure 6 show general agreement with flat surface results for the lower rms height surface, but appreciable differences for the rougher surface. Note object scattering returns centered around time  $-0.6$  ns show only minor deviations from the flat surface case since no surface scattering sources have been encountered (other than sidelobe contributions from later times.) Later time coherent returns in the rms height 1 cm begin to approach time domain returns with the object in free space (not plotted). Incoherent scattering contributions at zero degrees occur primarily at times after initial object returns, so that time domain object detection strategies would work well in this case. Incoherent returns show contributions from both surface only and object/surface

interactions, although surface only scattering dominates in the rougher case for most times. Initial object/surface incoherent interaction effects are found to be slightly time shifted from surface only scattering. This is consistent with the dominant four-path mechanism of a bistatic scattering from the object followed by a specular scattering from the rough surface, since a transmission through the object would result in a slight time delay. Object/surface interaction effects are observed to be more significant at later times, as would be expected for multiple object/surface interactions.

Figures 7 and 8 illustrate  $HH$  (plot (a)) and  $VV$  (plot (b)) time domain statistics for the rms height 3.58 mm and 1 cm cases, respectively. Similar observations regarding coherent fields are obtained in this case, with only slight differences from flat surface returns observed with rms height 3.58 mm while larger differences are observed in the rougher case as coherent fields approach those for an object in free space. Total incoherent returns show the time spreading associated with oblique observation of a rough surface, so that object scattering no longer occurs prior to rough surface returns, making target detection more difficult. As observed in Figures 4 and 5, incoherent scattering dominates coherent scattering for the rougher surface case, and surface only contributions generally are more significant than object/surface interactions even at later times. However, the  $HH$  polarized, low rms height surface shows object/surface interaction effects to exceed surface only contributions around time zero, consistent with the four-path model explanation.

## 6 Conclusions

The results of this study demonstrate some of the coherent and incoherent scattering effects which can occur in combined object/rough surface scattering problems. Coherent cross sections were found to resemble those for an object above a flat surface in the small roughness limit but to approach those for an object in free space as the roughness increased. A four-path model using a rough surface reduced reflection coefficient was found to match coherent cross sections well for normal incidence observation, although the accuracy was degraded at oblique observation where multiple object scattering effects can become more important. Incoherent scattered fields in both the time and frequency domains showed that both direct surface backscattering and object/surface

interaction terms can be important depending on the frequency, surface statistics, polarization, and scattering geometry. Incoherent object/surface interaction effects observed appear consistent with a four-path model interpretation in which the dominant contribution is from an object bistatic scattering followed or preceded by surface forward scattering. Thus both surface backscattering and forward scattering effects must be considered when analyzing returns from object above a rough surface. Further applications of these results and the iterative method of moments model include evaluation of approximate models for combined surface/object problems [5]-[9], as well as tests of target detection algorithms in the presence of rough surface clutter.

## 7 Acknowledgements

This work was sponsored by ONR contracts N00014-97-1-0541 and N00014-00-1-0399, NSF project ECS-9701678, and by a grant from Duke University as part of the OSD MURI on Humanitarian Demining. Use of the IBM SP system at the Maui High Performance Computing Center is acknowledged, sponsored by the Air Force Research Laboratory, Air Force Materiel Command under cooperative agreement F29601-93-2-0001. Opinions, interpretations, conclusions, and recommendations are those of the authors and are not necessarily endorsed by the United States Air Force, Air Force Research Laboratory, or the U.S. Government.

## References

- [1] He, J. Q., T. J. Yu, N. Geng, and L. Carin, "Method of moments analysis of electromagnetic scattering from a general three-dimensional dielectric target embedded in a multilayered medium," *Radio Science*, vol. 32, pp. 305–313, 2000.
- [2] Geng, N., M. A. Ressler, and L. Carin, "Wide-band VHF scattering from a trihedral reflector situated above a lossy dispersive halfspace," *IEEE Trans. Geosc. Rem. Sens.*, vol. 37, pp. 2609–2617, 1999.
- [3] Cui, T. J. and W. C. Chew, "Fast algorithm for electromagnetic scattering by buried 3-D dielectric objects of large size," *IEEE Trans. Geosc. Rem. Sens.*, vol. 37, pp. 2597–2608, 1999.

- [4] Johnson, J. T., “A study of the four-path model for scattering from an object above a half-space,” submitted to *Microwave Opt. Tech. Lett.*, 2001.
- [5] Zhang Y., Y. E. Yang, H. Braunisch, and J. A. Kong, “Electromagnetic wave interaction of conducting object with rough surface by hybrid SPM/MOM technique,” *PIER 22: Progress in Electromagnetics Research*, vol. 22, pp. 315–335, 1999.
- [6] Ishimaru, A., J. D. Rockway, and Y. Kuga, “Rough surface Green’s function based on the first-order modified perturbation and smoothed diagram methods,” *Waves in Random Media*, vol. 10, pp. 17–31, 2000.
- [7] Chiu, T. and K. Sarabandi, “Electromagnetic scattering interaction between a dielectric cylinder and a slightly rough surface,” *IEEE Trans. Ant. Prop.*, vol. 47, pp. 902–913, 1999.
- [8] Johnson, J. T., “Thermal emission from a layered medium bounded by a slightly rough interface,” accepted by *IEEE Trans. Geosc. Remote Sens.*, 2000.
- [9] Fuks, I. M. and A. G. Voronovich, “Wave diffraction by rough interfaces in an arbitrary plane-layered medium,” *Waves in Random Media*, vol. 10, pp. 253–272, 2000.
- [10] O’Neill, K., R. F. Lussky, and K. D. Paulsen, “Scattering from a metallic object embedded near the randomly rough surface of a lossy dielectric,” *IEEE Trans. Geosc. Rem. Sens.*, vol. 34, pp. 367–376, 1996.
- [11] Dogaru, T. and L. Carin, “Time-domain sensing of targets buried under a rough air-ground interface,” *IEEE Trans. Ant. Prop.*, vol. 46, pp. 360–372, 1998.
- [12] Tjuatja, S., A. K. Fung, and J. Bredow, “Radar imaging of buried objects,” *IGARSS’98*, conference proceedings, pp. 524–526, 1998.
- [13] Zhang, G. F., L. Tsang, and K. Pak, “Angular correlation function and scattering coefficient of electromagnetic waves scattered by a buried object under a two-dimensional rough surface,” *J. Opt. Soc. Am. A*, vol. 15, pp. 2995–3002, 1998.

- [14] A. V. der Merwe and I. J. Gupta, "A novel signal processing technique for clutter reduction in GPR measurements of small, shallow land mines," *IEEE Trans. Geosci. Remote Sensing*, vol. 38, pp. 2627–2637, 2000.
- [15] Pino. M. R., L. Landesa, J. Rodriguez, F. Obelleiro, and R. J. Burkholder, "The generalized forward-backward method for analyzing the scattering from targets on ocean-like rough surfaces," *IEEE Trans. Ant. Prop.*, vol. 47, pp. 961–969, 1999.
- [16] Sletten, M. A., D. B. Trizna, and J. P. Hansen, "Ultrawide-band radar observations of multipath propagation over the sea surface," *IEEE Trans. Ant. Prop.*, vol. 44, pp. 646–651, 1996.
- [17] Shtager, E. A., "An estimation of sea surface influence on radar reflectivity of ships," *IEEE Trans. Ant. Prop.* vol. 47, pp. 1623–1627, 1999.
- [18] Tsang, L., J. A. Kong and R. T. Shin, *Theory of Microwave Remote Sensing*, John Wiley and Sons, New York, 1985.
- [19] Tsang, L., C. H. Chan, K. Pak, H. Sangani, "Monte Carlo simulations of large scale problems of random rough surface scattering and applications to grazing incidence with the BMIA/canonical grid method," *IEEE Trans. Ant. Prop.*, vol. 43, pp. 851–859, 1995.
- [20] Johnson, J. T., R. T. Shin, J. A. Kong, L. Tsang, and K. Pak, "A numerical study of the composite surface model for ocean scattering," *IEEE Trans. Geosc. Remote Sens.*, vol. 36, pp. 72-83, 1998.
- [21] Draine, B. T. and P. J. Flatau, "Discrete-dipole approximation for scattering calculations," *J. Opt. Soc. Am. A*, vol. 11, pp. 1491–1499, 1994.
- [22] Flatau, P. J., "Improvements in the discrete-dipole approximation method of computing scattering and absorption," *Optics Letters*, vol. 22, pp. 1205–1207, 1997.
- [23] Barrett, R., M. Berry, T. Chan, J. Demmel, J. Donato, J. Dongarra, V. Eijkhout, R. Pozo, C. Romine, and H. van der Vorst, *Templates for the Solution of Linear Systems: Building Blocks for Iterative Methods*, available by *ftp* from *netlib2.cs.utk.edu*, 1993.

- [24] Johnson, J. T. and R. J. Burkholder, “Coupled canonical grid/discrete dipole approach for computing scattering from objects above or below a rough interface,” accepted by *IEEE Trans. Geosc. Rem. Sens.*, 2000.
- [25] Pak, K., L. Tsang, C. H. Chan, and J. T. Johnson, “Backscattering enhancement of electromagnetic waves from two dimensional perfectly conducting random rough surfaces based on Monte Carlo simulations,” *J. Optical Soc. of America*, vol. 12, pp. 2491–2499, 1995.
- [26] Johnson, J. T., R. T. Shin, J. A. Kong, L. Tsang, and K. Pak, “A numerical study of ocean polarimetric thermal emission,” *IEEE Trans. Geosc. Remote Sens.*, vol. 37, pp. 8–20, 1999.
- [27] E. Newman, *A User’s Manual for The Electromagnetic Surface Patch Code: Preliminary Version ESP5.0*, ElectroScience Laboratory, The Ohio State University, unpublished report, 1997.
- [28] Rice, S. O., “Reflection of electromagnetic waves from slightly rough surfaces,” *Commun. Pure Appl. Math*, vol. 4, pp. 361–378, 1951.
- [29] Voronovich, A. G., *Wave Scattering from Rough Surfaces*, Berlin: Springer-Verlag, 1994.
- [30] McDaniel, S. T., “Acoustic and radar scattering from directional seas,” *Waves in Random Media*, vol. 9, no. 4, pp. 537–549, 1999.
- [31] J. L. Salvati, C. C. Chen, and J. T. Johnson, “Theoretical study of a surface clutter reduction algorithm” *IEEE Geoscience and Remote Sensing Symposium*, conference proceedings, pp. 1460–1462, 1998.
- [32] *Maui High Performance Computing Center World Wide Web Site*, on the World Wide Web at [www.mhpcc.edu](http://www.mhpcc.edu).

## List of Figures

Figure 1: Geometry of problem

Figure 2: Average backscattered radar cross sections versus frequency for 0 degrees incidence (a) Coherent (b) Incoherent

Figure 3: Coherent backscattered radar cross sections versus frequency for 45 degrees incidence (a) HH (b) VV

Figure 4: Incoherent backscattered radar cross sections versus frequency for 45 degrees incidence (a) HH (b) VV

Figure 5: Comparison of rough surface incoherent backscattering with small slope approximation versus frequency (a) 0 degrees incidence (b) 45 degrees incidence

Figure 6: Envelope of time domain backscattered fields for 0 degrees incidence. (a) Surface rms height 3.58 mm (b) Surface rms height 1 cm

Figure 7: Envelope of time domain backscattered fields for 45 degrees incidence: surface rms height 3.58 mm (a) HH (b) VV

Figure 8: Envelope of time domain backscattered fields for 45 degrees incidence: surface rms height 1 cm (a) HH (b) VV

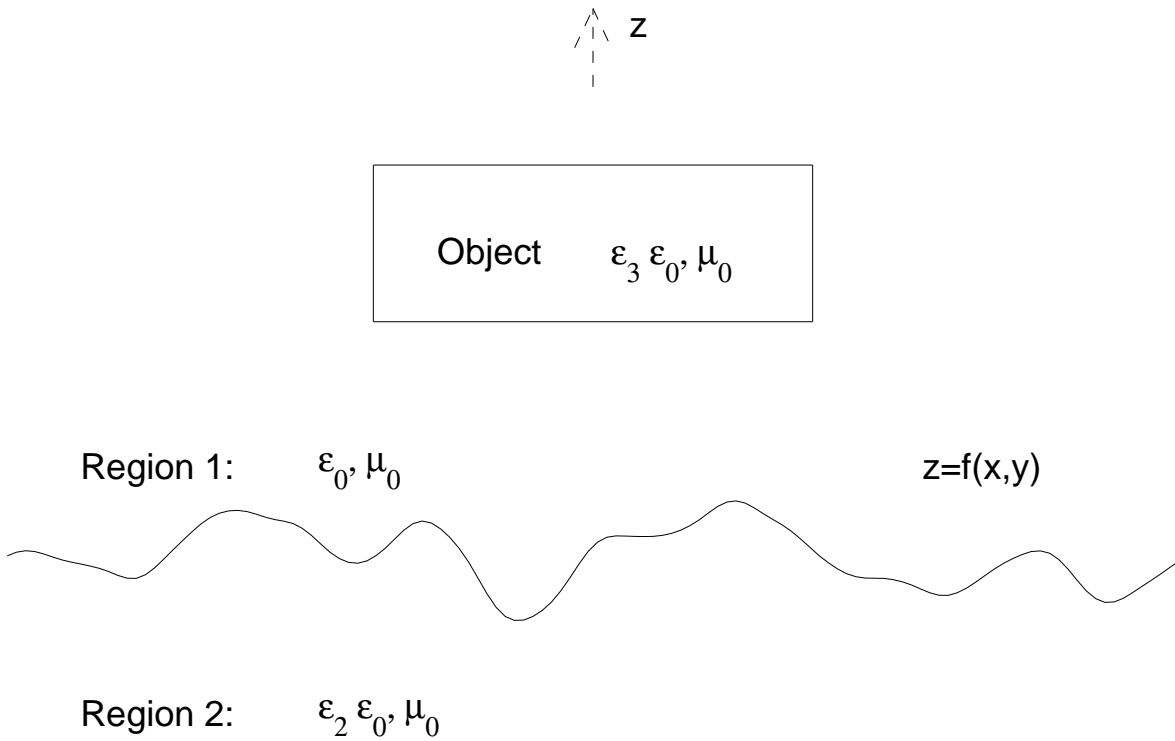


Figure 1: Geometry of problem

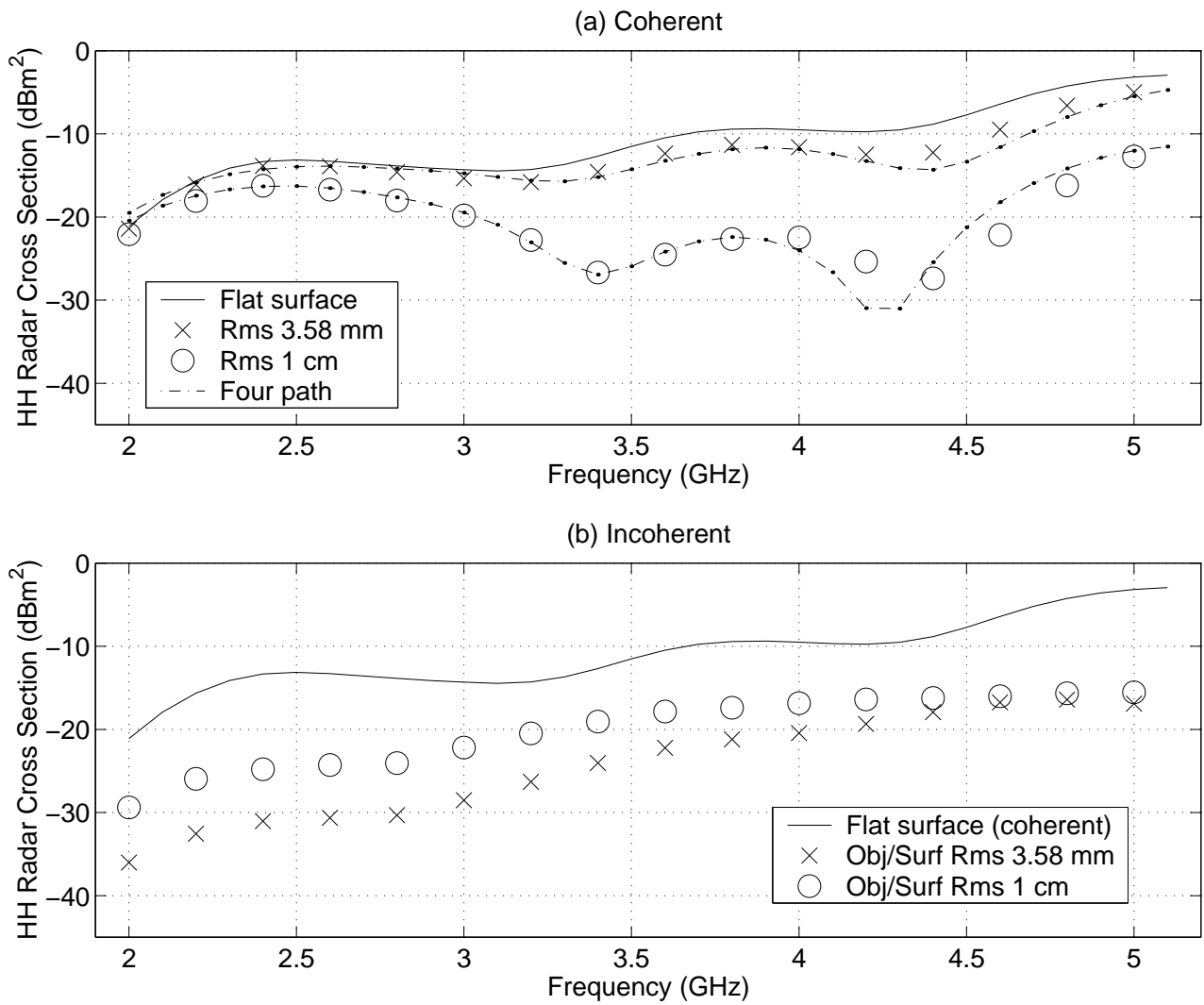


Figure 2: Average backscattered radar cross sections versus frequency for 0 degrees incidence (a) Coherent (b) Incoherent

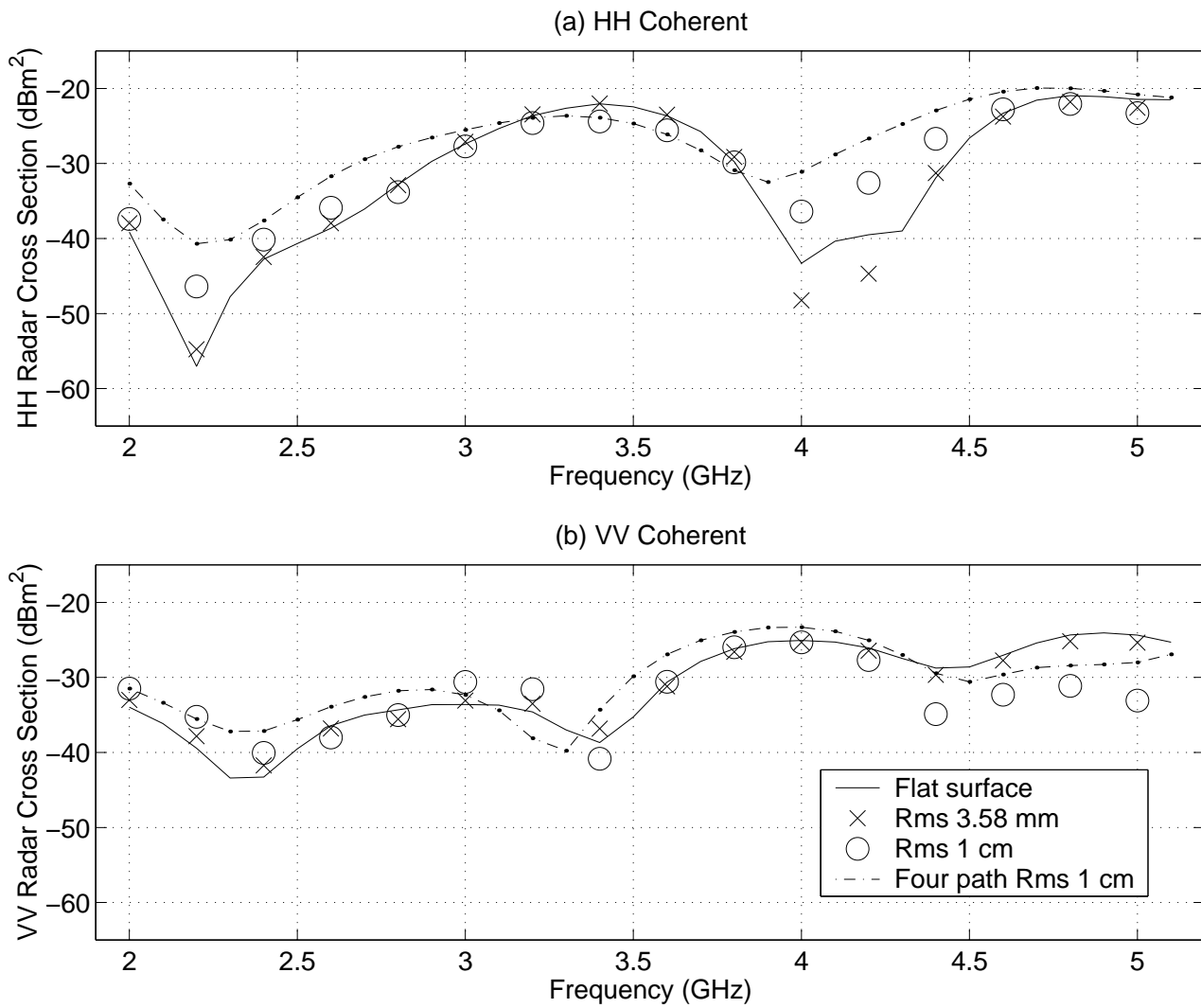


Figure 3: Coherent backscattered radar cross sections versus frequency for 45 degrees incidence (a) HH (b) VV

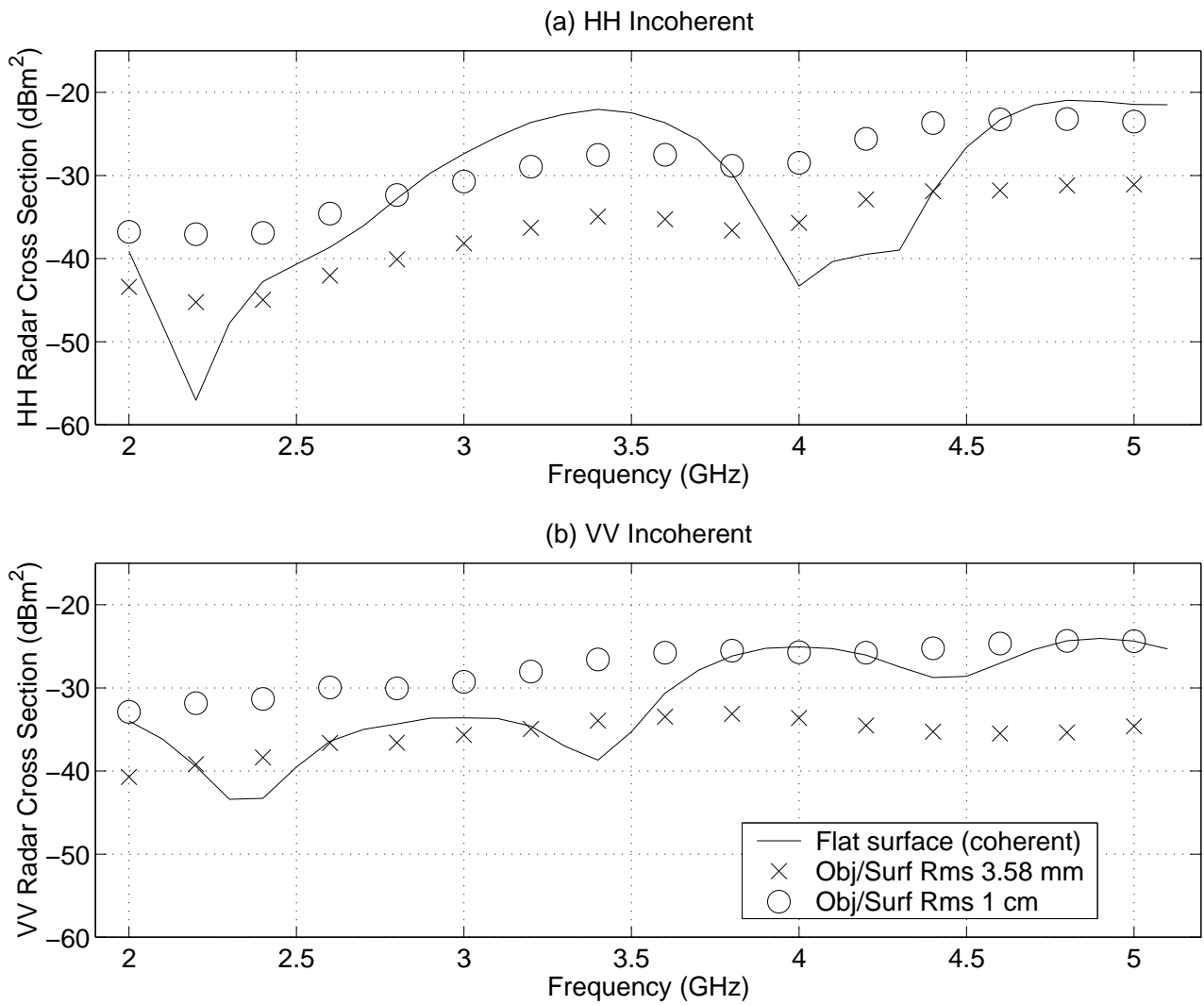


Figure 4: Incoherent backscattered radar cross sections versus frequency for 45 degrees incidence (a) HH (b) VV

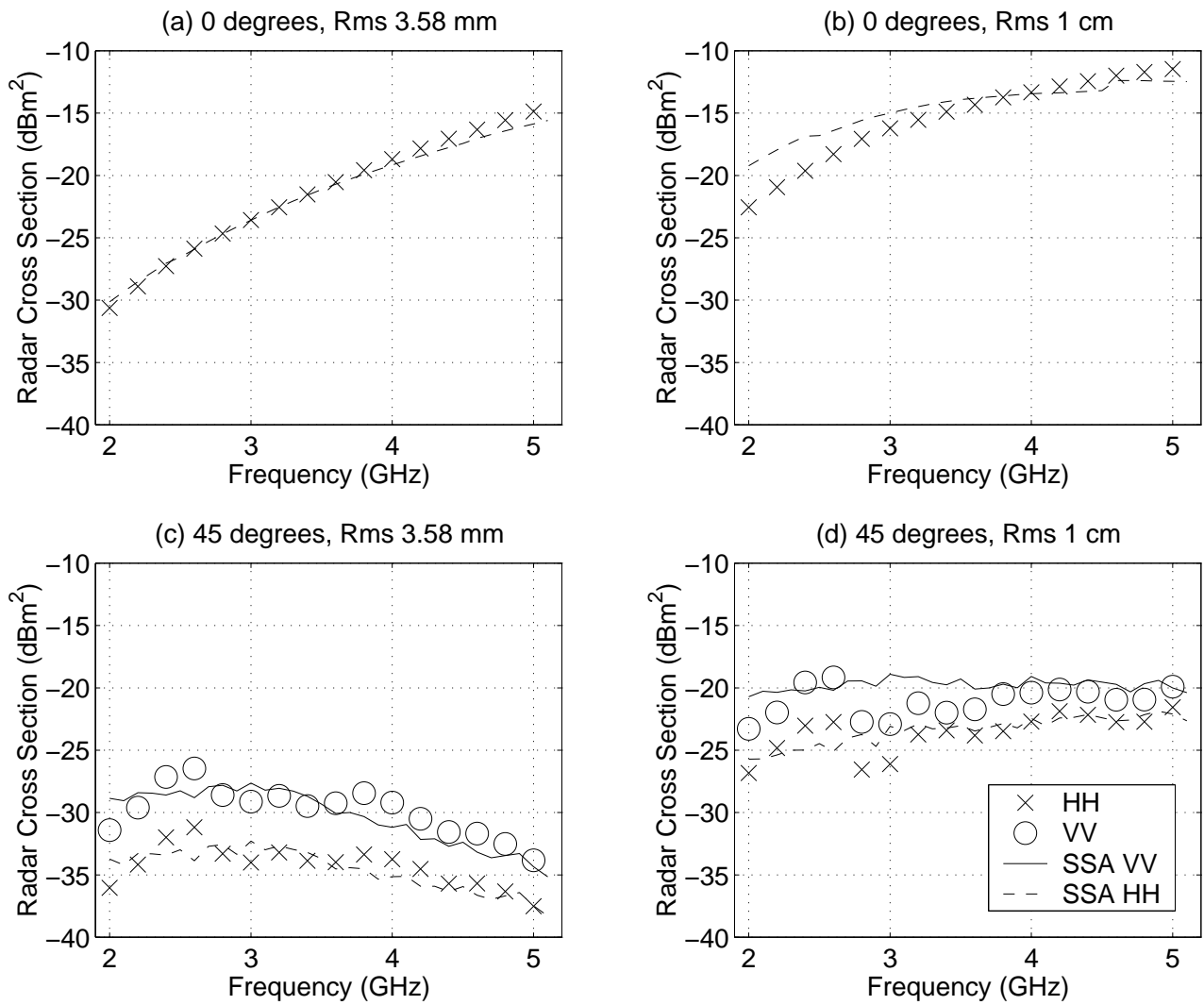


Figure 5: Comparison of rough surface incoherent backscattering with small slope approximation versus frequency (a) 0 degrees incidence (b) 45 degrees incidence

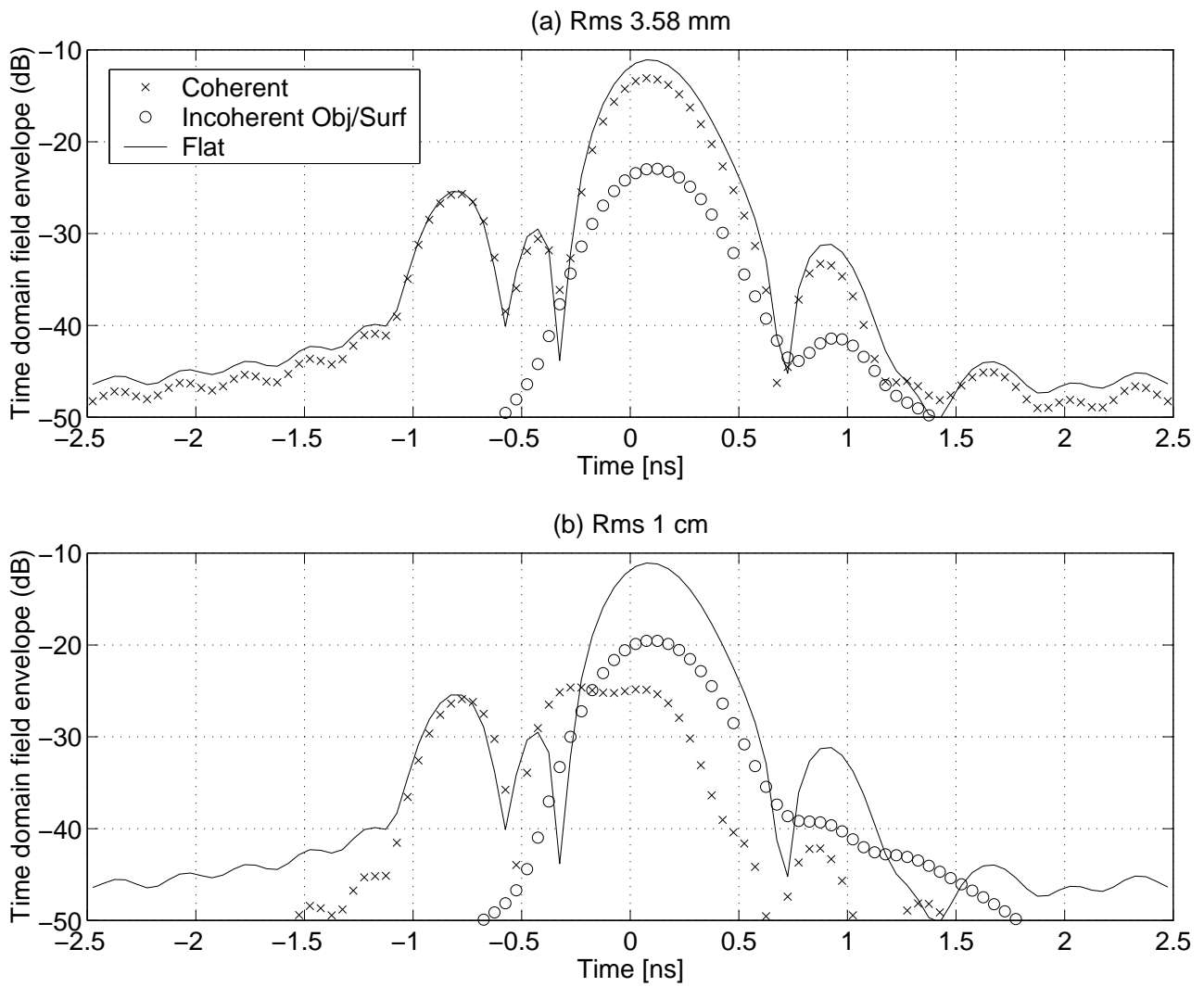


Figure 6: Envelope of time domain backscattered fields for 0 degrees incidence. (a) Surface rms height 3.58 mm (b) Surface rms height 1 cm

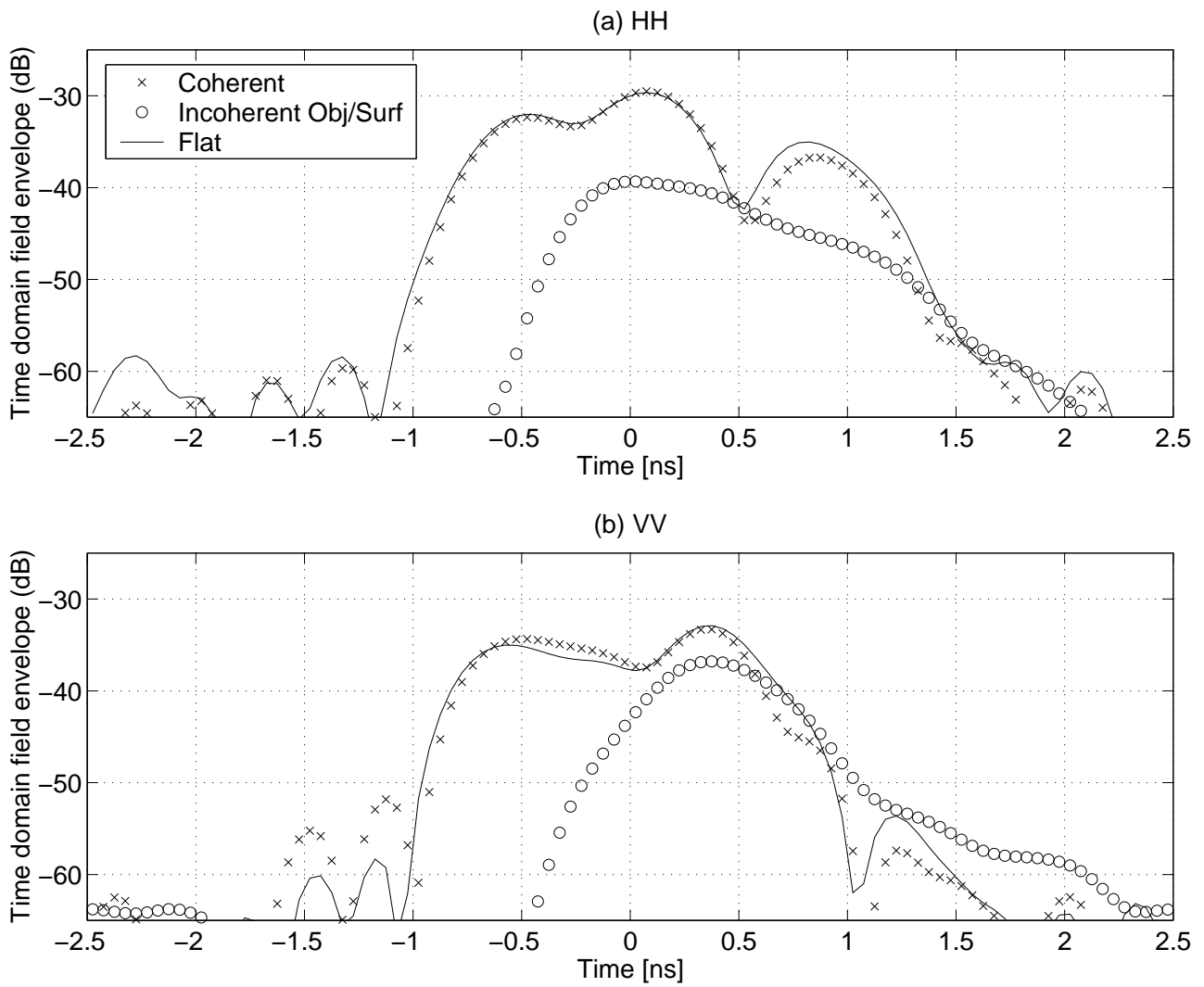


Figure 7: Envelope of time domain backscattered fields for 45 degrees incidence: surface rms height 3.58 mm (a) HH (b) VV

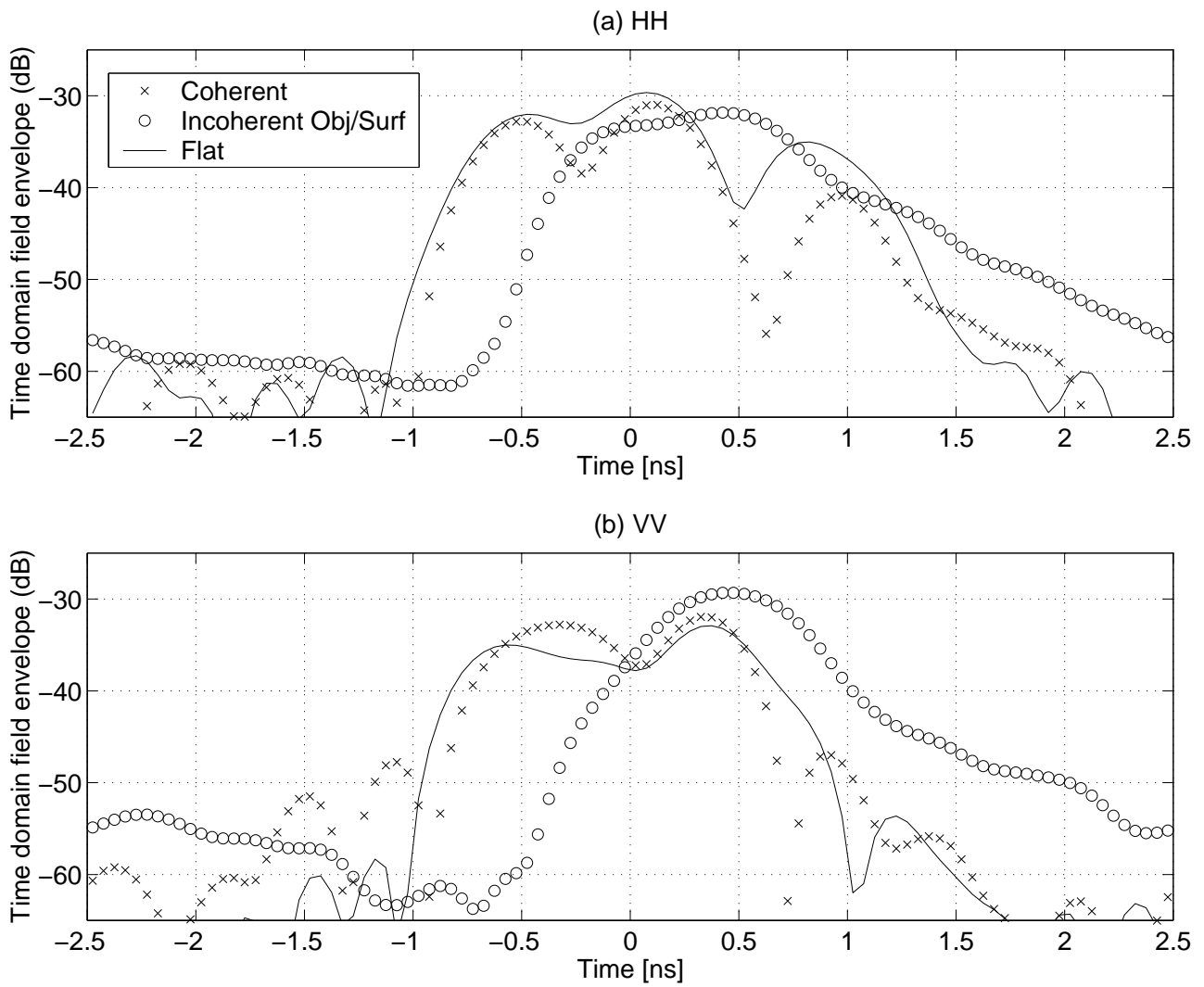


Figure 8: Envelope of time domain backscattered fields for 45 degrees incidence: surface rms height 1 cm (a) HH (b) VV